

# Effects of residual stresses and compressive mean stresses on the fatigue strength of longitudinal fillet-welded gussets

Jonas Hensel<sup>1</sup> · Thomas Nitschke-Pagel<sup>1</sup> · Klaus Dilger<sup>1</sup>

Received: 15 August 2014 / Accepted: 11 December 2015 / Published online: 12 January 2016  
© The Author(s) 2016, corrected publication 2021

**Abstract** Results from fatigue testing of small-scale specimens are widely used to study residual stress effects on fatigue of welded structures. It was observed from a literature that welding distortion may cover residual stress effects due to high-bending stresses from clamping. Here, presented are fatigue test results and results from residual stress measurements from welded longitudinal stiffeners in different residual stress conditions. The axial welding distortion was corrected for all samples by straightening reducing effects from clamping and making residual stress effects visible. It was found that the fatigue strength depends strongly on the stabilized residual stresses, especially at high numbers of load cycles. It could be shown that residual stresses at the weld toe either were far below the yield strength or were degraded mainly at the first load cycle but still have major effects. This was investigated at two stress ratios of  $R = -1$  and  $R = -3$ .

**Keywords (IIW Thesaurus)** Residual stresses · Fillet welds · Fatigue loading · Stress relaxation · Weld toes · Fatigue strength

## 1 Introduction

Residual stresses in steels are generated during manufacturing processes, such as welding, and are resulting from inhomogeneous

plasticity. Welding residual stresses in regular construction steels with ability to phase transformation have two main sources [1]. The first source of residual stresses is hindered shrinkage of heterogeneously heated zones during cooling. The magnitude of those tensile residual stresses from hindered shrinkage depends on the heat input, the heat conductivity, the coefficient of thermal expansion of the welded metals, and the stiffness of the structure. The restraint of the heterogeneously heated zones by colder adjacent material leads to local yielding and generates heterogeneous strains. High restraint may lead to high tensile residual stresses. In engineering practice, tensile residual stresses near the weld may be lowered by the second mechanism. Transforming material volumes, for instance in the heat-affected zone of steel welds, increase packing density while undergoing  $\gamma$ - $\alpha$ -transformation. This volume increase reduces tensile residual stresses from shrinkage depending on the cooling rate. High cooling rates are normally generating martensite or bainite microstructure whereas low cooling rates normally result in ferrite-pearlite microstructure. The temperature at which the phase transformation occurs has major effect on the magnitude of compressive residual stresses from hindered volume expansion. This is due to mechanical properties at elevated temperatures. The final residual stress state is always a result from compressive residual stresses due to phase transformation and tensile residual stresses from shrinkage.

The experimental determination of the fatigue strength of welded components relies generally on small-scale laboratory specimens. Residual stress effects are also often investigated using this type of samples such as butt welds, cruciform joints, transverse stiffener, or overlap joints. But in fact, these linear-shaped welds show low stiffness perpendicular to the welding direction resulting in low shrinkage constraints. Consequently, the residual stresses perpendicular to the welding direction (which is normally the loading direction) are usually small. The scalability of results from linear weldments obtained in

---

Recommended for publication by Commission XIII - Fatigue of Welded Components and Structures

✉ Jonas Hensel  
j.hensel@tu-braunschweig.de

<sup>1</sup> Institute of Joining and Welding, TU Braunschweig, Braunschweig, Germany

laboratory scale is thus difficult. Real structures often show much higher stiffness perpendicular to the welding direction allowing for higher residual stresses and thus a different fatigue behavior under cyclic loading. One of the few sample types that show comparable residual stresses in laboratory scale and in real structures is the longitudinal stiffener, Fig. 2. This specimen shows considerably high tensile residual stresses below the weld. At this sample type, one can observe the interaction of the two mentioned mechanisms of residual stress generation. The magnitude of tensile residual stresses from shrinkage is lowered by effects from phase transformation at the locations of crack initiation [2]. In specimen depth, one can find high residual stresses in the magnitude of the yield strength.

Residual stresses are possibly subject to relaxation since their magnitude is always limited by the yield strength of the material. In consequence, residual stresses are considered to be more stable in case of high-strength steels, respectively, martensite or bainite microstructure than in low-strength ferrite-pearlite steels. The mechanisms of residual stress relaxation are generally described by [3]. Specific investigations on welded high- and low-strength steel showed that the major residual stress relaxation occurs at initial loading in cases where the sum of residual stresses and load stresses exceeded the static yield strength [4, 5]. In cases of cyclic softening, one should also expect further residual stress relaxation with increasing load cycles until the sum of residual stresses, and load stresses no longer exceed the cyclic yield strength [6].

Residual stresses and welding distortion are inseparably connected to each other. The welding distortion of small-scale specimens, such as longitudinal stiffeners, is minimized by low heat input and optimized weld order. However, welding distortion of small-scale specimens can never be fully avoided due to the lack of geometric stiffness. In consequence,

the clamping of distorted samples in test rigs may result in additional bending stresses depending on the specimen length and thickness and the stiffness of the test environment. The resulting fatigue strength may be affected by those uncontrolled extra loading in unpredictable matter. An example of which is given in Fig. 1 [7]. Longitudinal stiffeners made of fine-grained low-carbon construction steel S355NL ( $R_e = 390$  MPa) were tested in as welded and thermally stress-relieved condition at a stress ratio of  $R = -1$  ( $R = \sigma_{\min} / \sigma_{\max}$ ). The fatigue test results of both conditions were comparable both in short- and long-term fatigue life. According to IIW-guidelines, one would expect higher fatigue life of annealed samples due to the thermal relaxation of tensile residual stresses from welding. Although tensile residual stresses were proven in the entire crack path of as welded samples, there was no benefit from annealing observed here. The reason for this behavior is the increased welding distortion after the annealing process (the definition of welding distortion used here is the axial angle between both ends of the specimens). Here, it was reported that the distortion angle was increased by annealing from  $0.4^\circ$  to  $0.8^\circ$ . This led to constant higher bending stresses in case of higher distortion angles and thus reduced fatigue strength. In consequence, fatigue test results of as welded and annealed specimens are not representative for the effects of residual stresses at a stress ratio of  $R = -1$ . Concluding this study, this effect is a phenomenon of laboratory testing. If residual stresses shall be investigated, welding distortion must be controlled or accounted for in the process of result transfer from laboratory scale to real-welded structures.

The given example shows strongly the necessity of the knowledge of precise specimen conditions if testing in laboratory scale. Many investigations on the influence of mean

**Fig. 1** S-N data from longitudinal stiffeners tested with welding distortion in as welded and annealed condition at  $R = -1$  [7]

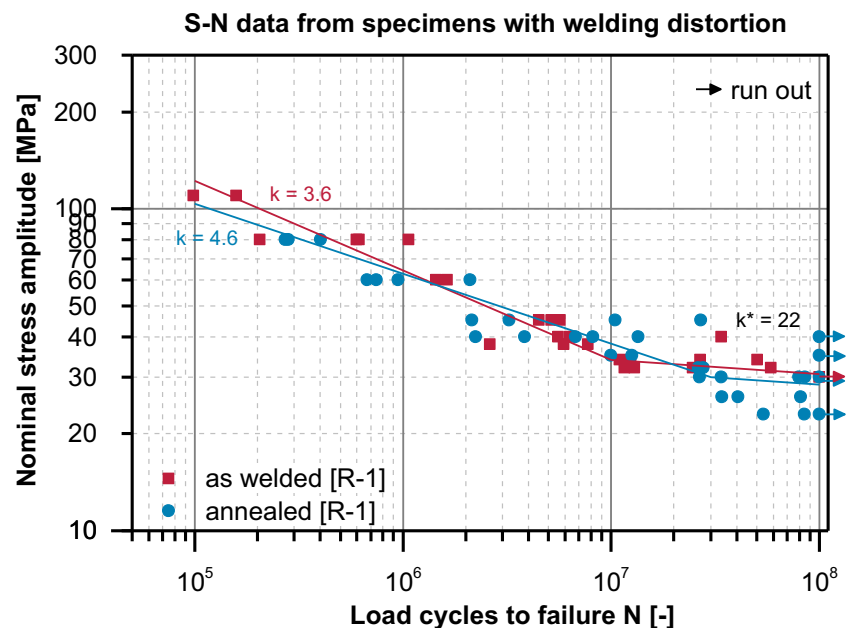
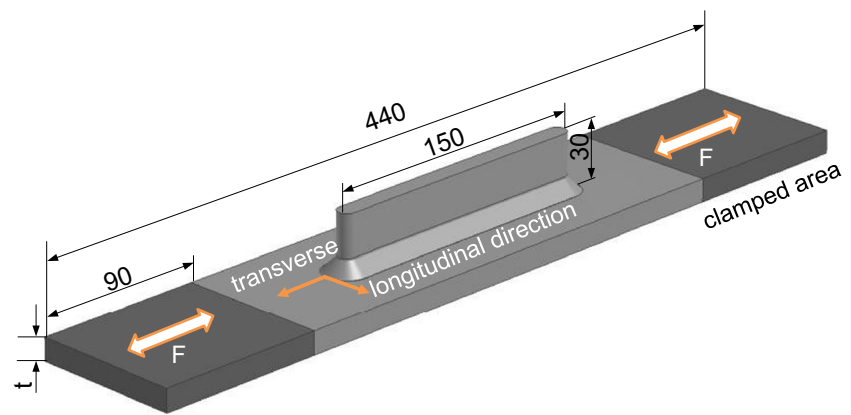


**Fig. 2** Specimen geometry used for fatigue testing. Reference for residual stress (transverse and longitudinal) directions at the location of crack initiation referring to the welding direction [22]



stresses or residual stresses, even those used as data base for design guidelines [8–11], do not account for such specimen details. In consequence, results should be questioned if no information on specimen conditions such as welding distortion, residual stresses, weld geometry, or other parameters are given in the literature.

The consideration of additional bending stresses according to the literature can be made for instance by a mean stress correction and adjustment of the nominal stress amplitudes according to local  $R$  ratios. However, these techniques did not work out for this test series shown before. Reasons may be the comparable short sample length of 400 mm which resulted in high inelastic-bending stresses at the weld notch or just the simplicity of the amplitude adjustment approach. It could not be clarified whether it is suitable to treat deflection-controlled bending stresses as load controlled mean stresses. Additionally, this technique assumes a certain mean stress dependency, for instance according to [12] or [13], which in reality is normally unknown.

## 2 Experimental work

The samples used here in the presented investigation were axial-loaded longitudinal stiffeners made of a fine-grained low-carbon construction steel (S355NL, grade 1.0546). The geometry of the samples is shown in Fig. 2. The specimen's

length was 440 mm with a width of 80 mm. The areas used for clamping was 90 mm from both ends. The thickness  $t$  was 10 mm, respectively, 12 mm. The samples failed from the short sides of the stiffeners from the weld toe. All residual stress measurements were performed at those locations. The nomenclature used for the directions of the residual stress components (longitudinal and transverse residual stresses) is oriented at the welding direction as usual for linear welds. The welding direction at the short sides of the stiffeners is oriented perpendicular to the loading direction.

Fatigue testing was undertaken with different specimen conditions at constant amplitude loading. Residual stress states were varied from high tensile to compressive residual stresses. An overview over the specimen conditions used is given in Table 1. Specimens were tested as welded, annealed, shot-peened as well as after pre-stressing (tension). The annealing was conducted at 600 °C for 30 min using argon-shielding gas. The cooling was carried out to 200–250 °C in the oven and showed cooling rates of approximately 120 K/h. Shot-peening was performed at OSK Kiefer GmbH, Oppurg, Germany, with an Almen intensity of 0.4 A. The shot-peening medium was S230 using 4-bar pressure and 200 % coverage. Pre-stressed samples were loaded closely to the nominal yield strength by one-load cycle. The overload applied corresponded to 98 % of the yield strength of the base metal.

Fatigue tests were made at stress ratios of  $R = -1$  and  $R = -3$ . These stress ratios were chosen for the reason that

**Table 1** Overview on test series and weld details (FJP: full joint penetration; PJP: partial joint penetration)

Test series	Stress Ratio $R$	S355NL	Weld detail	Number of samples tested	Flank angle $\alpha$ ISO 5817 (mean)	Axial distortion (mean)
As welded	-1	Material 1	PJP	16	135°	0.09°
Annealed	-1	Material 1	PJP	24	135°	0.08°
Shot-peened	-1	Material 2	FJP	12	140°	0.13°
Pre-stressed	-1	Material 1	FJP	12	142°	0.15°
As welded	-3	Material 1	PJP	15	134°	0.11°
Annealed	-3	Material 1	PJP	16	135°	0.10°
Shot-peened	-3	Material 2	FJP	13	141°	0.20

**Table 2** Chemical composition of the materials used (in mass percent %)

S355NL (1.0546)				Material 1				<i>t</i> = 12 mm			
C	Si	Mn	P	S	Cr	Cu	Mo	Ni	V	CET	CE
0.197	0.468	1.107	0.010	<0.001	0.033	0.213	<0.001	0.209	<0.001	0.325	0.417
S355NL (1.0546)				Material 2				<i>t</i> = 10 mm			
C	Si	Mn	P	S	Cr	Cu	Mo	Ni	V	CET	CE
0.156	0.411	1.389	0.010	<0.001	0.033	0.294	0.017	0.058	<0.011	0.301	0.404

residual stress may have severe influence only at low tensile, zero, or even compressive mean stresses. These stress ratios are also of interest because many lightweight structures are optimized regarding typical fatigue critical locations. These critical weld details are typically loaded under tensile mean stresses. But structural optimization or post-weld-treatment methods may lead to a shift of the fatigue relevant weld details to structural parts loaded under lower stress ratios.

Two different materials of S355NL with a thickness of 12 and 10 mm were used. The welding of the longitudinal attachment was performed either as single layer fillet weld (partial joint penetration—PJP) or as three-layer full penetration weld (full joint penetration—FJP). The specimen geometry was determined by means of a laser sensor. The geometry was used to identify welding distortion as well as the flank angle  $\alpha$  according to ISO 5817. PJP welds showed slightly steeper flank angles than FJP welds. The definition used for the welding distortion angle was the intersection angle of both clamped ends of the samples. The welding distortion was corrected in order to minimize effects from clamping as described in Section 3.1. It was decreased from more than  $1.0^\circ$  to a range from  $0.09^\circ$  to  $0.15^\circ$ .

The chemical composition of the two materials used is shown in Table 2. Material 1 showed a higher carbon content of 0.197 % in comparison to 0.156 %. The weldability of both materials was given without preheating due to carbon equivalents CET of 0.325, respectively, 0.301. The composition of both materials fulfilled requirements according to EN 10025.

The filler metal used was EN ISO 14341-A-G4Si1. The welding was performed by means of six-axis robot using GMA welding process. Start and stop of the welding was set at the long sides of the stiffeners. The energy input used was chosen to approximately 0.9–1.2 kJ/mm. Cooling times  $t_{8/5}$  from 800 to 500 °C at the short sides of the stiffeners were determined by means of type K thermocouples to 4–7 s.

Table 3 shows the static strength of the materials used. Material 1 showed higher yield strength  $R_e$  of 390 MPa in

**Table 3** Mechanical properties of the materials used

S355NL	Material 1	<i>t</i> = 12 mm	S355NL	Material 2	<i>t</i> = 10 mm
Yield strength $R_e$	390 MPa		Yield strength $R_e$	356 MPa	
Ultimate strength $R_m$	568 MPa		Ultimate strength $R_m$	517 MPa	

comparison to material 2 with 356 MPa. The ultimate strengths  $R_m$  were determined to 568, 517 MPa, respectively.

The micrographs and measured Vickers hardness of the weld details investigated are given in Fig. 3. Vickers hardness HV1 was measured in a grid (distance of measuring points 0.3 mm×0.3 mm) using the ultrasonic impedance method (UCI). The UCI device was calibrated in advance with a standard Vickers test. The location of fatigue crack initiation for both sample types was the weld toe (and not the weld root) at the continuous sheet metal at the end of the longitudinal stiffener. The hardness of the base material 1 was determined to 170 HV1 and to 161 HV1 for material 2. The weld metal hardness was measured to 230 HV1 for fillet-welded samples and to approximately 210 HV1 for fully penetrated welds resulting from local annealing by multi-layer welding. The hardness at the weld toe notch for both weld details was determined to approximately 280 to 320 HV1. This high hardness is resulting from the low heat input at the ends of the stiffeners going along with a short cooling time  $t_{8/5}$ .

## 2.1 Correction of welding distortion

The correction of the welding distortion of the samples was performed carefully by means of a three-point bending device, Fig. 4. The goals that needed to be satisfied in the straightening process were achieving samples with defined bending stresses from clamping of insignificant magnitude without disturbing the residual stress field at the location of fatigue crack growth. The plastic zone was therefore located in a certain distance to the weld toe test section. Measurements of residual stresses by means of X-ray diffraction before and after the correction of the welding distortion were undertaken and proved that the residual stresses within 20 mm of the weld toe were not affected.

Measurements with strain gauges proofed the success of the correction for welding distortion. Clamping strains in the net section between weld and clamping could be reduced from more than 500  $\mu\text{m/m}$  in the distorted as welded condition to less than 100  $\mu\text{m/m}$  after correction. One side effect of this set up is a misalignment of the test section at weld toe and the clamping section. This misalignment was determined to 0.2 mm causing second-order bending of small magnitude depending on the load amplitude.

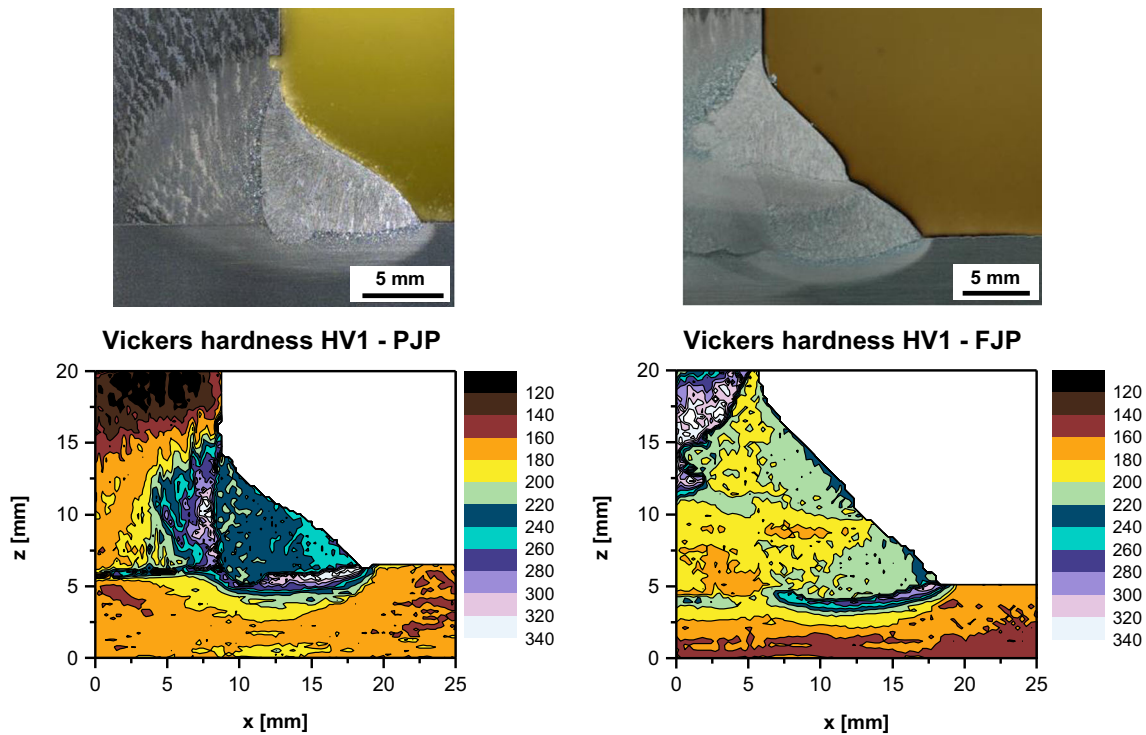


Fig. 3 Micrograph and Vickers hardness (HV1) from as welded file-welded joint (PJP) and from fully penetrated joint (FJP)

2.2 Initial residual stresses

The generation of residual stresses in welded longitudinal stiffeners was determined by means of several methods and different sample conditions already before [2]. The typical residual stress field below the weld in as welded condition can be seen in Fig. 5. Residual stresses shown here were determined by means of neutron diffraction at HZB, Berlin along the fatigue crack path A-A'. Details on the neutron diffraction experiment used can be found in [14]. Tensile residual stresses were proven below the entire weld in both directions showing a tension maximum 3-mm below the surface. The highest tension residual stresses were proven transverse to the welding direction corresponding to the axial loading direction in fatigue testing. Although not shown here, it was proven by means of X-ray diffraction methods that thermal stress relieve reduced residual stresses to less than 50 MPa.

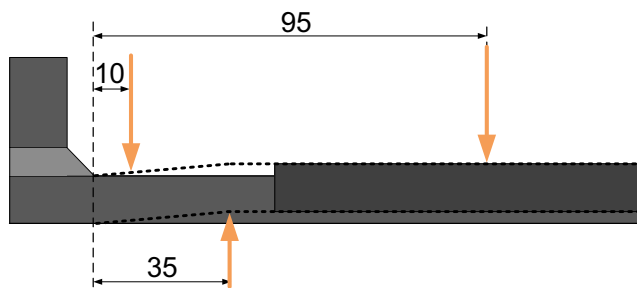


Fig. 4 Set up of the process used for the correction of welding distortion [22]

2.3 Residual stress relaxation at R=-1

Residual stresses at the surface were determined by means of X-ray diffraction. Diffraction analysis was used to study cyclic residual stress relaxation for samples in different residual stress conditions. The load level was chosen in accordance to the lower finite life regime resulting from S-N testing (Section 3.5). Next to initial residual stresses at  $N=0$ , the measurements were repeated at the same locations after  $N=1$  and  $N=10,000$  load cycles. Residual stresses were determined for both directions, transverse and longitudinal to the welding direction at the short sides of the stiffeners. Residual stresses in shot-peened samples and in as welded samples were also measured after  $N=100,000$  load cycles.

Residual stresses were calculated from measured  $\{211\}$ -Fe interference lines by means of the  $\sin^2\Psi$ -method. Eleven  $\Psi$ -angles, a collimator size of 2 mm and Cr-radiation were used here. Residual stresses were measured along a line in loading direction beginning at the weld toe at the short sides of the stiffeners with direction into the base metal. The measuring points near the weld toe were located closely to each other in a distance of 0.5 mm. The distance in the base metal was 1 to 2 mm. The full width at half maximum (FWHM) is given next to calculated residual stresses in the following as well. The FWHM corresponds to the dislocation density at the measuring points and can be used a measure for the quality of the residual stress analysis. Especially one can precisely evaluate the accuracy of the positioning of the measuring points at the sample surface. This information is of high value if samples



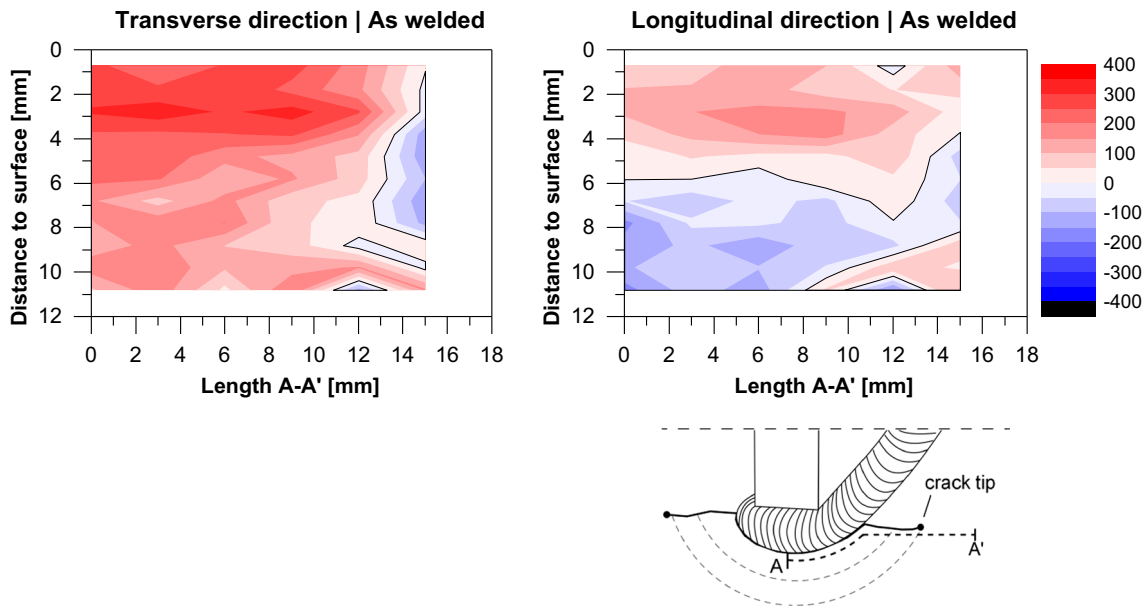


**Fig. 5** Residual stress field below the weld toe of a longitudinal stiffener in as welded condition [14]. Presented are residual stresses transverse to the welding direction (top left) and parallel to the welding direction (top right) in depth along the crack path A-A' (right)

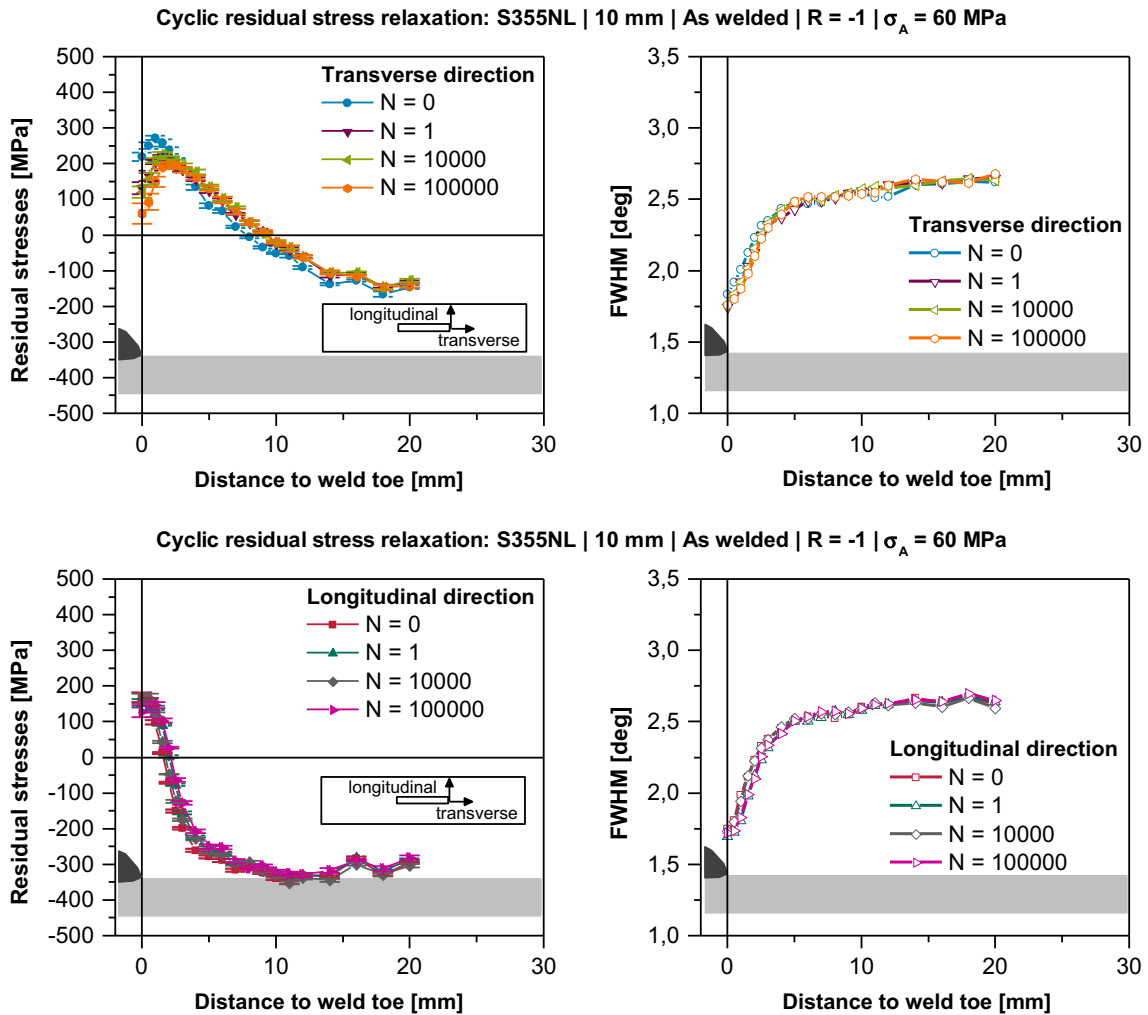


**Fig. 6** S355NL, as welded sample. Cyclic residual stress relaxation at  $R = -1$  with  $\sigma_A = 60$  MPa and full widths at half maximum values from X-ray diffraction measurements

are re-mounted in a diffractometer for instance after mechanical loading in a load frame.

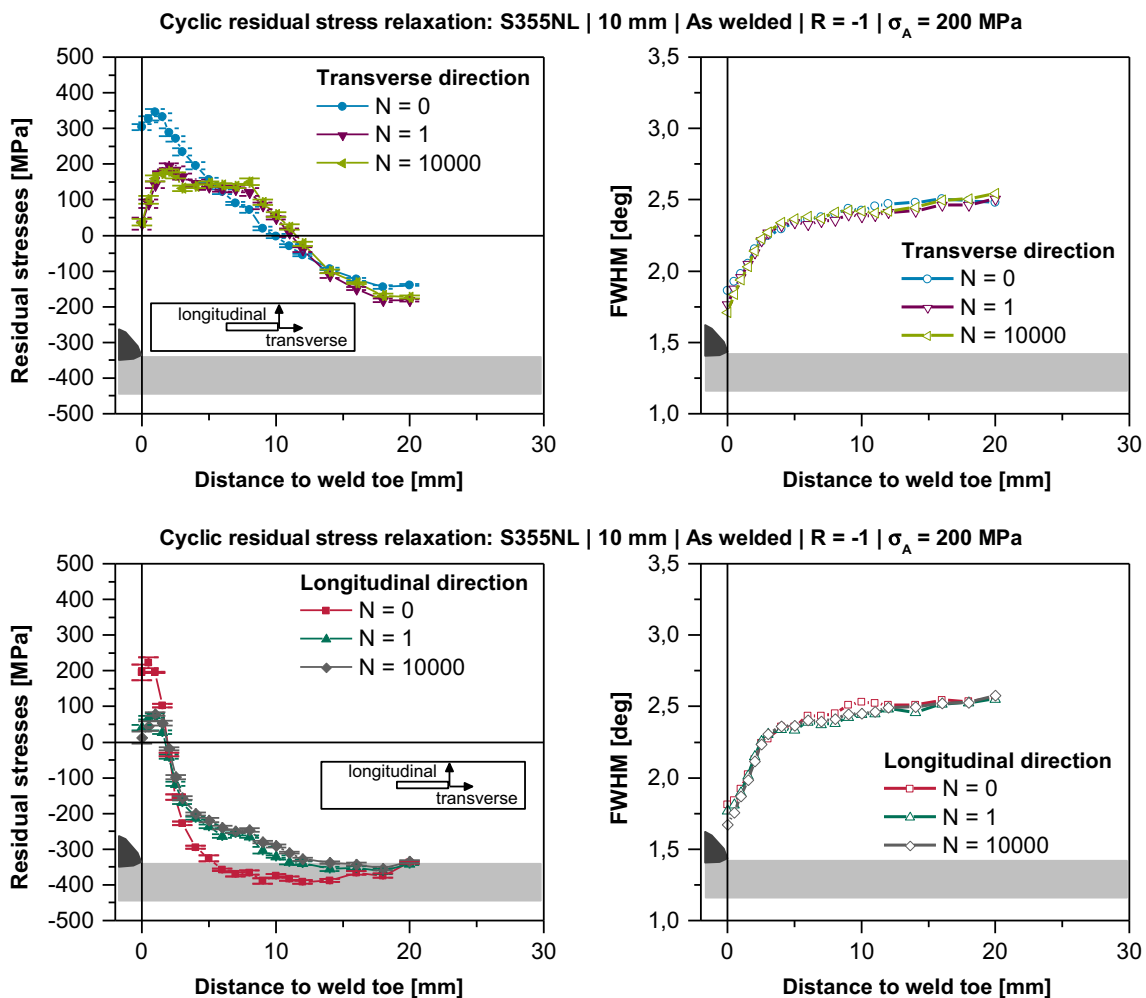
Cyclic residual stress relaxation was investigated at a stress ratio of  $R = -1$  for as welded, shot-peened and pre-stressed samples. The results are given below.

Figure 6 shows residual stresses from an as welded sample. The sample was loaded with a nominal stress amplitude of  $\sigma_A = 60$  MPa. Initial residual stresses transverse to the welding direction showed at  $N=0$  (initial condition) 200 MPa at the weld toe which increased to 270 MPa in a distance of 2-mm to the weld toe. After  $N=1$  load cycle residual stresses at the notch were degraded to 110 MPa due to the stress concentration of the weld. The maximum shifted slightly further into the base metal and was reduced to 100 MPa. After following cyclic loading to  $N=100,000$ , slight relaxation of residual stresses to 60 MPa was found at the weld toe. Longitudinal to the welding direction, no residual stress relaxation was observed. At the weld toe, residual stresses with a magnitude of 160 MPa were observed initially and after cyclic loading. Residual stresses dropped into compression in a distance of

approximately 3-mm to the weld toe. Compressive residual stresses were observed in a distance of approximately 10-mm to the weld toe in both directions. These compressive residual stresses were generated in advance of welding by the clean blasting process to remove the mill scale.

FWHM remained for all three load stages constant. The clean-blasted base metal showed values of approximately  $2.5^\circ$ . The FWHM dropped to approximately  $1.8$  at the weld toe due to the heat treatment from the welding process. This showed that effects from clean-blasting, like work hardening and the generation of compressive residual stresses, were neutralized by the welding process.

Residual stress relaxation was expected at higher stress amplitudes. A nominal load amplitude of 200 MPa was chosen to evaluate the degree of residual stress relaxation at  $R = -1$ , see Fig. 7. Initially comparable residual stresses as shown in Fig. 6 were detected. After  $N = 1$  load cycle, residual stresses at the weld toe as well as at the maximum were degraded considerably. Transverse to the welding direction residual stresses at the weld toe were degraded to 10 MPa and to



**Fig. 7** S355NL, as welded sample. Cyclic residual stress relaxation at  $R = -1$  with  $\sigma_A = 200$  MPa and full widths at half maximum values from X-ray diffraction measurements

200 MPa at the maximum. Longitudinal to the welding direction residual stresses were also degraded at the weld toe to 10 MPa and to 80 MPa at the maximum. Further loading did not lead to further relaxation. FWHM values remained stable during loading.

It should be mentioned that this load amplitude of 200 MPa is considerably high in terms of fatigue strength. Cyclic loading of such magnitude normally ends in low-cycle fatigue regime, compare Section 3.5.

Another set of samples was tested in pre-stressed condition. The pre-stressing was done close to the yield strength of the base metal with a force amplitude of 282 kN. Residual stresses were determined initially, after pre-loading and after initially cyclic loading with stress amplitudes of 120 MPa at  $R=-1$ , see Fig. 8. It can be seen from this figure that tensile residual stresses both transverse and longitudinal to the loading direction were degraded completely. Directly at the weld one could find compressive residual stresses of  $-70$  MPa in both directions. Residual stresses as found after pre-loading remained stable

during further cyclic loading to  $N=10,000$  load cycles. The residual stresses directly at the weld toe were controlled by X-ray measurements using a collimator of 0.8-mm diameter. No significant derivation compared to the use of a 2.0 mm was found.

Shot-peening generated compressive residual stresses and led to work hardening in the surface layer of the metal. Higher compressive residual stresses with almost  $-300$  MPa were observed here in comparison to clean blasted samples, see Fig. 9 (left). Compressive residual stresses of  $-400$  MPa could be found in the shot-peened base metal up to distance of 5-mm to the weld toe. Directly at the weld toe and in the heat-affected zone, compressive residual stresses were initially less distinctive with magnitudes between  $-200$  and  $-300$  MPa. The accessibility for shot peening seemed to be more difficult close to the weld for this specimen type due to geometric constraints. Compressive residual stresses transverse to the welding direction were degraded by first load cycle ( $\sigma_A=80$  MPa) from  $-200$  to  $-180$  MPa and further degraded to  $-130$  MPa by the next 10,000 load cycles. In longitudinal

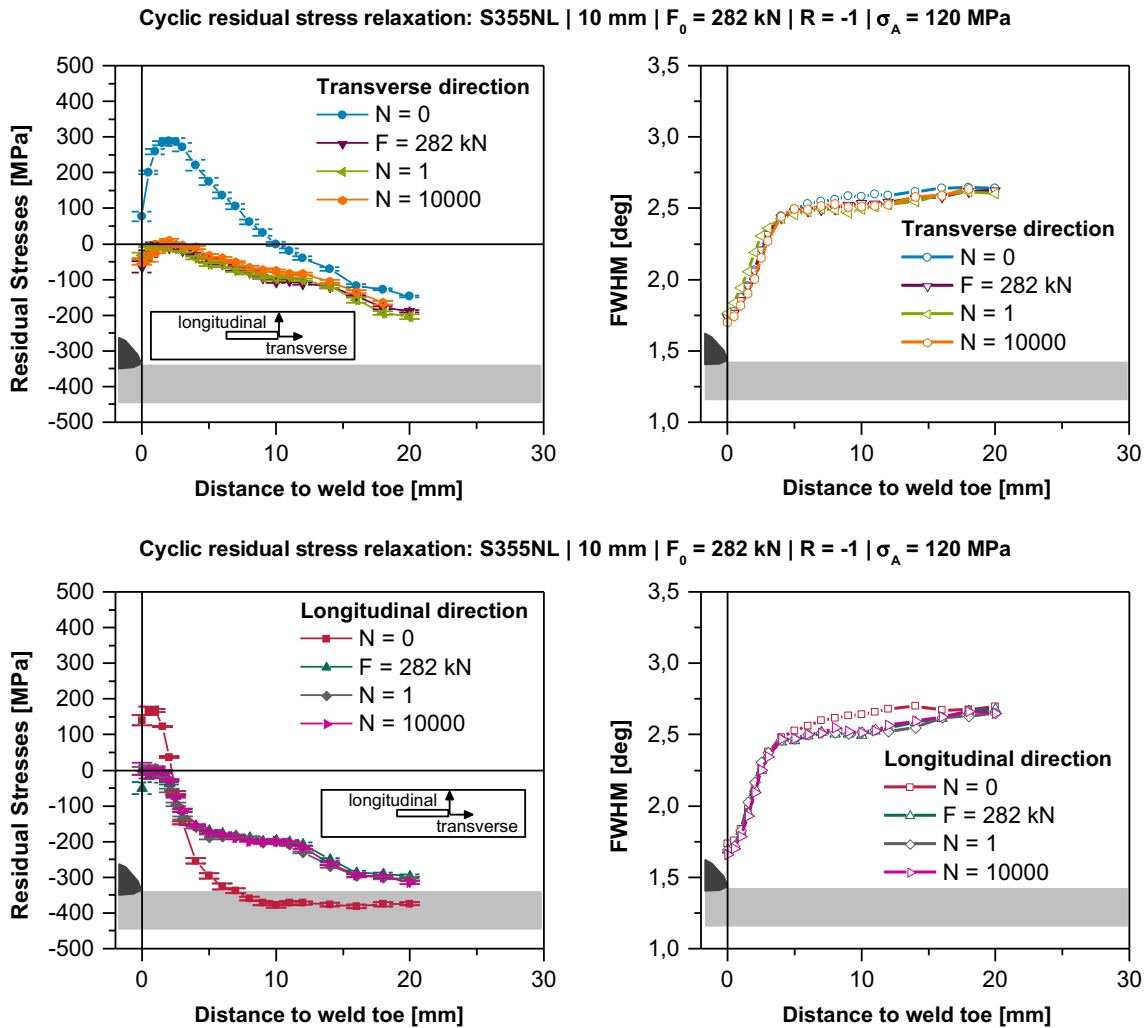


**Fig. 8** S355NL, pre-stressed sample to 282kN (98 % of  $R_c$ ). Cyclic residual stress relaxation at  $R=-1$  with  $\sigma_A=120$  MPa and full widths at half maximum values from X-ray diffraction measurements



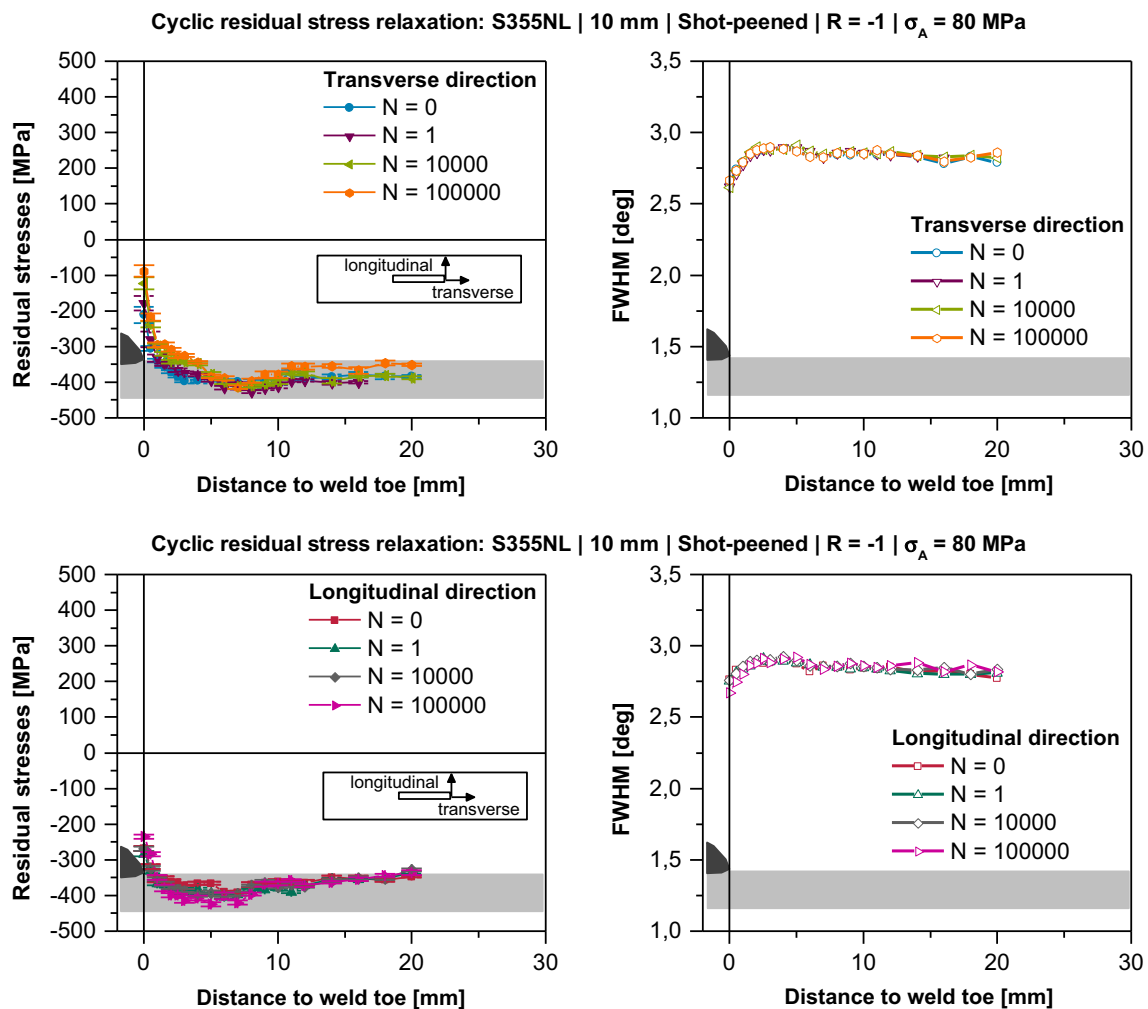


**Fig. 9** S355NL, shot-peened sample. Cyclic residual stress relaxation at  $R = -1$  with  $\sigma_A = 80$  MPa and full widths at half maximum values from X-ray diffraction measurements

direction, there was no relaxation observed. At higher numbers of load cycles ( $N = 100,000$ ), residual stresses transverse to the welding direction were further degraded to  $-90$  MPa at the weld toe. Also in the base metal, some degradation could be observed. Transverse to the welding direction, residual stresses were not changed significantly.

The FWHM referred to the work hardening resulting from the shot-peening process. The base metal showed values close to  $2.8^\circ$ ; whereas, the FWHM at the weld toe was  $2.6^\circ$ . This implies that the weld toe was less treated by shot peening than the base metal (Fig. 9, right).

#### 2.4 Residual stress relaxation at $R = -3$

Cyclic residual stress relaxation at a stress ratio of  $R = -3$  was also investigated next to residual stress behavior at zero mean stress as described above.

Residual stresses from samples as welded were studied at load stress amplitudes of 100 and 200 MPa. Figure 10 shows almost stability of residual stresses both transverse and

longitudinal to the welding direction at stress amplitudes of 100 MPa. Relaxation of small degree from 110 to 60 MPa was observed transverse to the welding direction at the weld toe. This degradation was observed at the first load cycle. FWHM values showed similar results as described for Fig. 6.

Another sample was loaded to higher nominal stress amplitudes of 200 MPa. Interestingly, Fig. 11 showed compressive residual stresses of  $-180$  MPa at the weld toe in initial condition transverse to the welding direction. These compressive residual stresses can be explained by a more distinctive heat-affected zone probably resulting from deviations in the welding process. This can also be concluded from FWHM values near the weld toe. In comparison to FWHM for instance from Fig. 6 or Fig. 10, it can be seen here that the width of the reduced FWHM at the weld toe is considerably wider. This points to a wider heat-affected zone, for instance from higher heat input. However, the first load cycle reduces compressive residual stresses at the weld to  $-30$  MPa which remained stable during further loading up to 10,000 load cycles. Tensile residual stresses longitudinal to the welding direction were

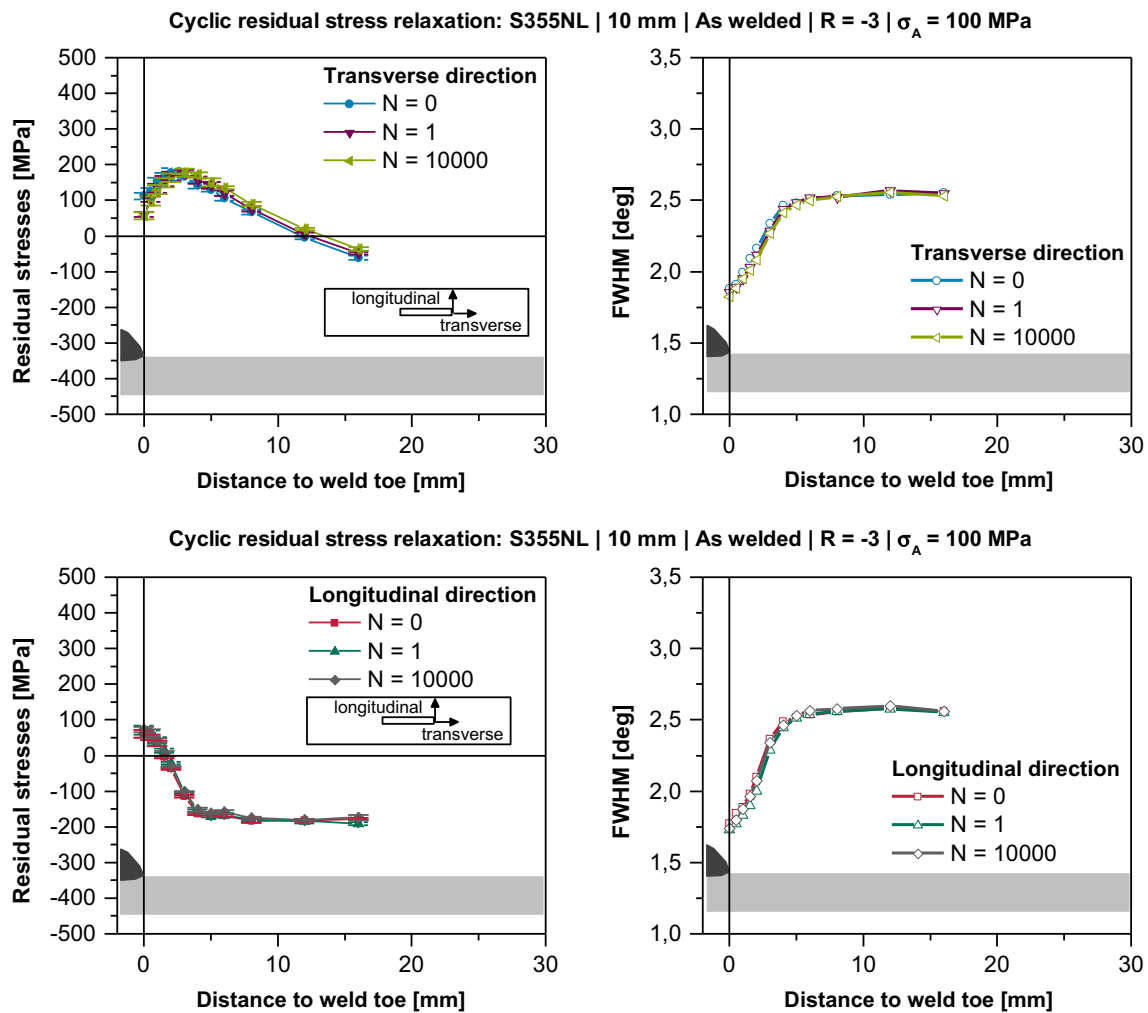


**Fig. 10** S355NL, as welded sample. Cyclic residual stress relaxation at  $R = -3$  with  $\sigma_A = 100$  MPa and full widths at half maximum values from X-ray diffraction measurements [22]

slightly relaxed by the first load cycle as well. Initially, 120 MPa was measured which was reduced to 80 MPa. The FWHM remained constant during cyclic loading.

Residual stresses from a shot-peened sample were studied at  $R = -3$  as well, Fig. 12. Initially, comparable residual stress conditions were observed as described for Fig. 9. Residual stress relaxation was observed transverse to the welding direction at the first load cycle ( $\sigma_A = 100$  MPa). Further loading to 10,000 load cycles did lead to residual stress degradation of small degree. But at higher numbers of load cycles of  $N = 100,000$ , cyclic relaxation transverse to the welding direction was found. There was also slight relaxation observed longitudinal to the welding direction. FWHM values determined transverse to the welding direction were degraded slightly from  $2.8^\circ$  to  $2.7^\circ$  at the first load cycle.

## 2.5 Fatigue testing results

Related to the specimen conditions and the investigations on cyclic residual stress relaxation described above, fatigue

testing was performed at  $R = -1$  and  $R = -3$ . All samples were controlled to be straight (axial distortion less than  $0.2^\circ$ ) before fatigue testing. Effects from clamping for all tested specimens were proven to be small and comparable.

At  $R = -1$ , samples were tested as welded, annealed, shot-peened, and pre-stressed, Fig. 13. The run-out criterion was chosen between 15 and 50 million load cycles. Samples as welded showed the lowest fatigue strength both in finite life and long-term fatigue life regime. The declination of the S-N was determined to  $k = 3.2$  by means of a regression analysis in direction of  $N$  without consideration of run-outs. The 50 % probability of failure of the fatigue strength at  $N = 2,000,000$  load cycles was determined to a nominal stress amplitude of 40 MPa. Annealing led to considerably higher fatigue strength at  $N = 2,000,000$  load cycles of 63 MPa. The declination  $k$  was determined to 3.1. Even higher fatigue strength was determined for pre-stressed samples. The nominal stress amplitude at  $N = 2,000,000$  load cycles was 109 MPa. The three mentioned S-N curves also showed run outs at very different load amplitude levels. The fatigue strength was increased by

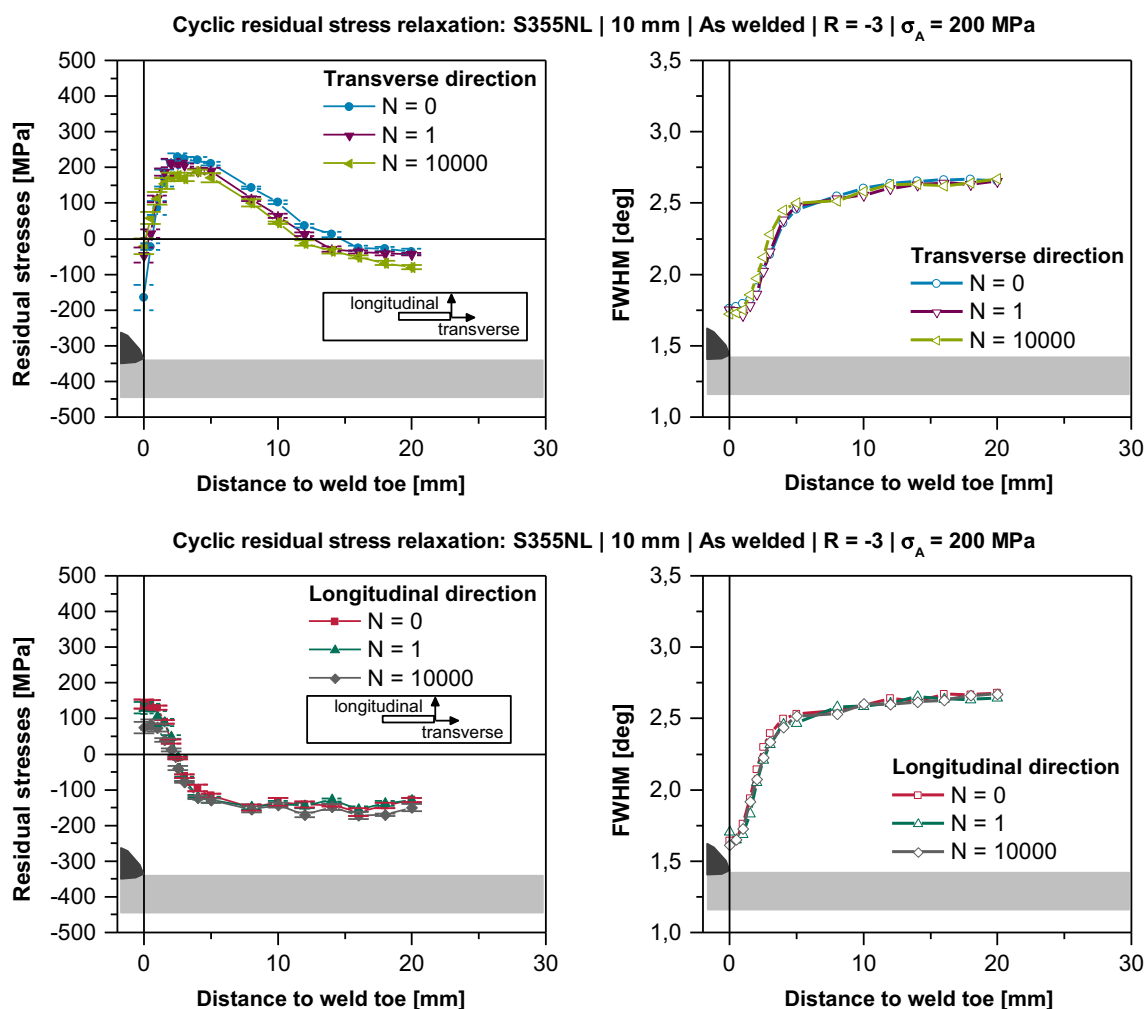


**Fig. 11** S355NL, as welded sample. Cyclic residual stress relaxation at  $R = -3$  with  $\sigma_A = 200$  MPa and full widths at half maximum values from X-ray diffraction measurements

annealing and pre-stressing both in finite life and in long-term fatigue life regime. Interestingly, shot-peened samples showed compared to as welded samples similar fatigue strength in finite life regime but significant higher fatigue strength in long-term fatigue life. The run-outs were tested at significantly higher stress levels. Consequently, the long-term fatigue strength was considerably higher due to a knee point position at a low number of load cycles (approximately  $N \approx 1,000,000$ ). The improvement factor from as welded to shot-peened samples at  $N = 10,000,000$  load cycles was determined to approximately  $(\sigma_{A, \text{shot peened}} / \sigma_{A, \text{as welded}}) \approx 2$ .

At  $R = -3$ , samples were tested as welded, annealed, and shot-peened up to  $N = 15,000,000$  load cycles, Fig. 14. As welded samples showed the lowest fatigue strength of 42 MPa at  $N = 2,000,000$  load cycles. Annealed samples showed significantly higher fatigue strength than as welded samples. The nominal stress amplitude at  $N = 2,000,000$  load cycles was determined to 98 MPa corresponding to an improvement factor larger than 2. Shot-peened samples showed

comparable behavior at  $R = -3$  and at  $R = -1$ . The fatigue strength at finite life was similar to as welded samples. But run-outs were tested at high stress levels leading to a knee point position at a low number of load cycles ( $N = 1,000,000$ ). By this, fatigue strength in long-term fatigue life ( $N > 10,000,000$ ) was almost doubled compared to as welded condition.

The fatigue strength of shot-peened samples at  $R = -3$  is comparable to thermally stress-relieved specimens in long-term fatigue life. The fatigue strength of shot-peened samples at high numbers of load cycles at  $R = -1$  was even higher than of annealed ones.

### 3 Discussion

Welding distortion was found to affect the fatigue strength in an unpredictable matter. The objective of this investigation was the evaluation of residual and mean stress effects on the fatigue strength of welded samples without effects from

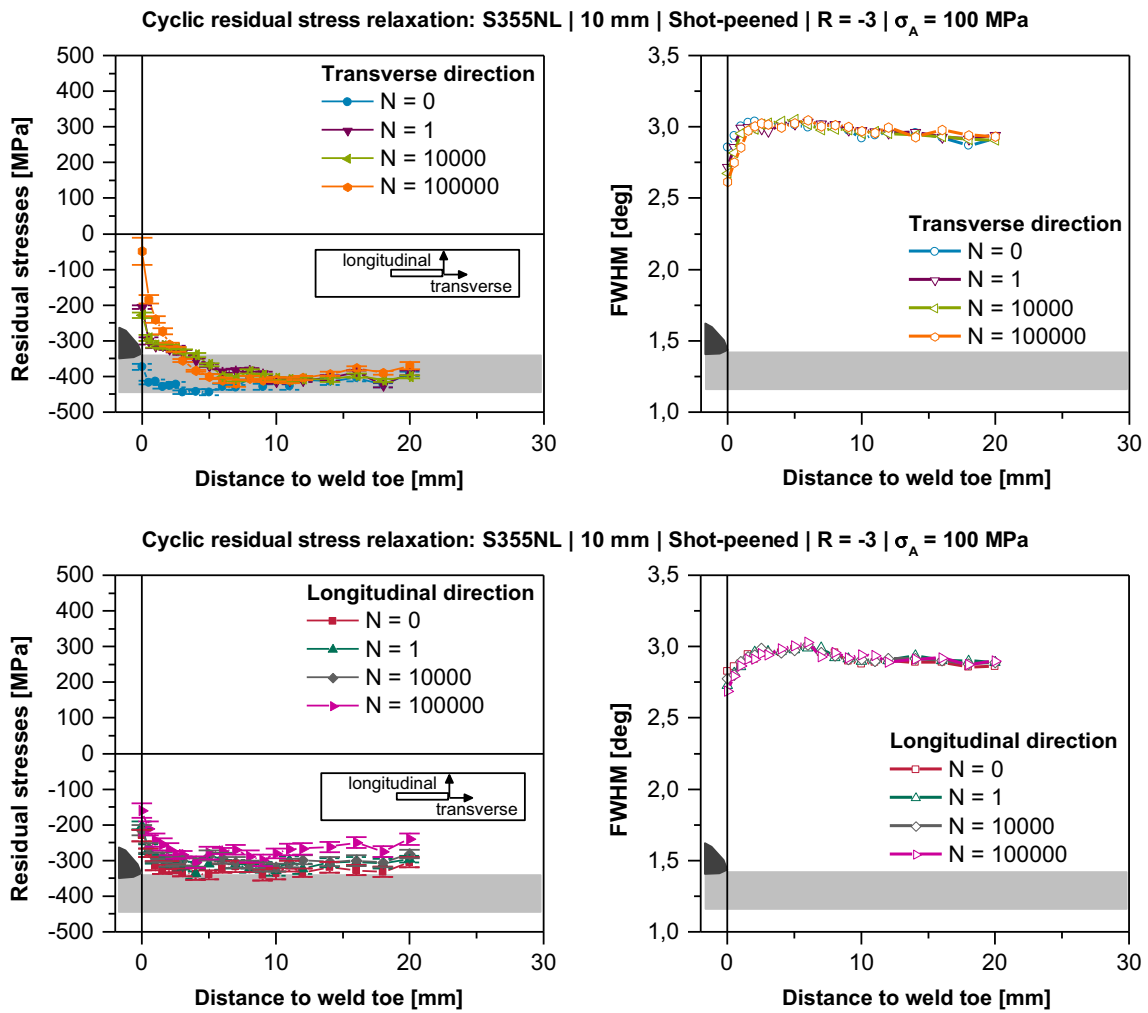


**Fig. 12** S355NL, as welded sample. Cyclic residual stress relaxation at  $R = -3$  with  $\sigma_A = 100$  MPa and full widths at half maximum values from X-ray diffraction measurements

**Fig. 13** S-N data from specimens tested at stress ratio  $R = -1$  to failure (distortion corrected)

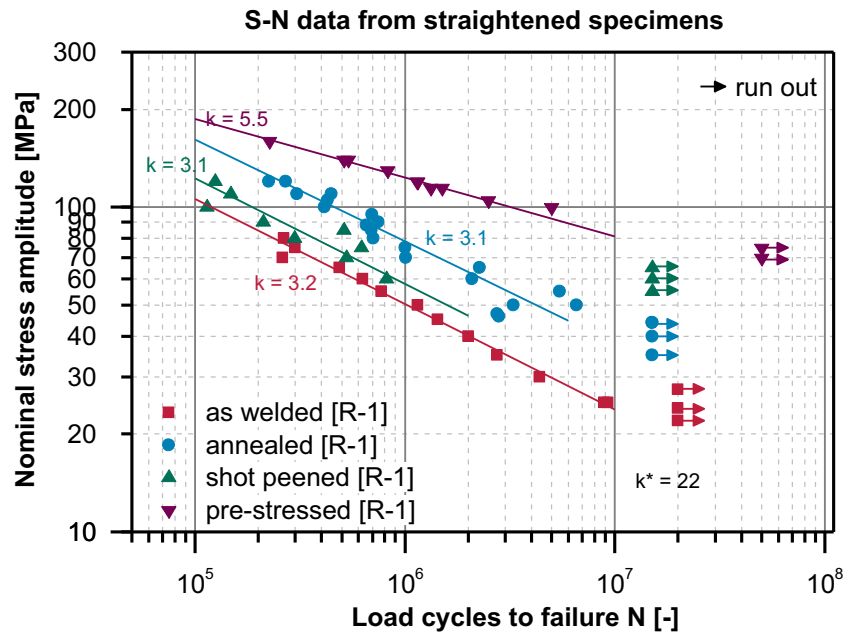
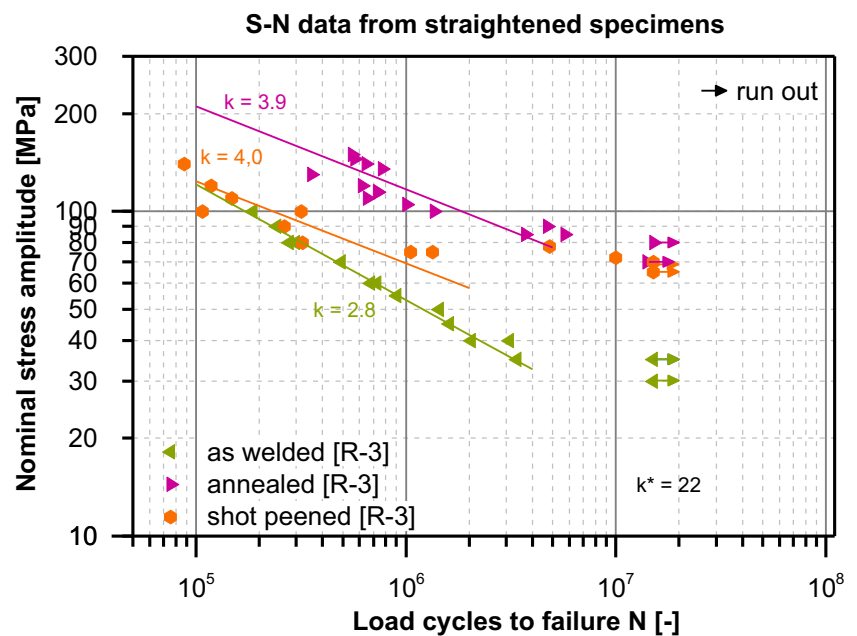


**Fig. 14** S-N data from specimens tested at stress ratio  $R=-3$  to failure (distortion corrected)



welding distortion. It was observed that residual stress relaxation in as welded samples mainly occurs at the first load cycle. Even small load amplitudes at  $R=-1$  may lead to residual stress degradation at the weld toe in cases where residual stresses are comparable high. This was observed for tensile residual stresses in as welded condition. This is in accordance to the literature. Thermal stress relieve led to considerable improvement of the fatigue strength. This could be observed in contrast to the fatigue test data shown in Fig. 1. The main reason for this was found to be the reduction of clamping stresses by correcting welding distortion. Clamping stresses covered residual stress effects in case of distorted samples although the distortion was low in terms of welding technology. Similar improvement of the fatigue strength of annealed samples was observed for fatigue testing with compressive mean stresses ( $R=-3$ ). The improvement was even slightly higher than in case of  $R=-1$ . This shows a mean stress dependence of stress-relieved samples whereas the fatigue strength of as welded samples was comparable at both stress ratios. The high improvement of the fatigue strength is a result of the thermal degradation of tensile residual stresses not only at the weld toe but also through specimen depth. At the surface, stabilized residual stresses were proven to be relatively low (about 25 % of the yield strength) resulting from either phase transformation effects or from relaxation at the first load cycle. The depth distribution of high-tensile residual stresses as welded remarkably affects fatigue strength. Pre-stressing up to the yield strength led to compressive residual stresses at the notch. Further, it could be expected to relax tensile residual stresses over depth as well and to generate compressive residual stresses even in depth direction. As result it was observed that the fatigue strength of pre-stressed samples at  $R=-1$  was

even higher than after thermal stress relieve. Compressive residual stresses at the notch significantly improved the fatigue strength by a factor of 3.4 at  $N=10,000,000$  load cycles but also in finite life. It could be shown that compressive residual stresses from pre-stressing were stable at subsequent constant amplitude loading.

At  $R=-1$  and  $R=-3$ , shot-peened samples showed a tendency to cyclic residual stresses relaxation. However, compressive residual stresses of considerable magnitude remained at the weld toe in case of small load amplitudes. This could be concluded from the shape of the S-N curve as well as from residual stress measurements. At high stress levels, fatigue strength of shot-peened samples was comparable to those of as welded samples. This was also observed earlier [15–17]. The observation of cyclic relaxation of compressive residual stresses at high stress amplitudes is a new contribution to this. At lower stress amplitudes S-N curves of as welded and shot-peened samples differed significantly. Compressive residual stresses from shot peening became effective at stress amplitudes below approximately 60 MPa at  $R=-1$  and below 70 MPa at  $R=-3$ . At compressive mean stresses, the residual stress relaxation of shot-peened samples was observed at the first load cycle as well as after cyclic loading. Compressive residual stresses from shot peening lowered the yield strength at the first load cycle in compression at  $R=-3$ .

#### 4 Conclusion and outlook

Longitudinal stiffeners were investigated in fatigue testing regarding residual stress and mean stress influence. Residual stresses were varied from tension to compression by post-



weld treatment. Compressive residual stresses were generated by shot peening and pre-stressing. Next to the fatigue testing also residual stress relaxation was investigated at stress amplitudes corresponding to the finite life regime. For all samples, the welding distortion was corrected in order to reduce effects from clamping due to welding distortion. It was shown that small-scale samples with small welding distortion are suitable to study residual stress effects. Although the effect of clamping stresses on fatigue strength seems to be obvious, it must be stated that only few publications refer to exact sample conditions. In particular, collections of fatigue data (for instance [8–11]) used for the definition of design of S-N curves and the derivation of improvement factors, for instance for thermal stress relieve, do not contain this information either.

It was found from the fatigue testing and residual stress measurements:

- Thermal stress relieve led to a significant improvement of the fatigue strength about a factor of 2.0 at  $R=-1$  and 2.3 at  $R=-3$  in comparison to as welded condition. As welded samples showed no mean stress sensitivity.
- Pre-stressing to the nominal yield strength led to further improvement of the fatigue strength at  $R=-1$  compared to as welded and annealed. The improvement from as welded to pre-stressed condition was determined to 3.4 and from annealed to pre-stressed condition to 1.8.
- Shot-peening led to an improvement of the fatigue strength in high-cycle fatigue at both tested stress ratios. The fatigue strength in finite life regime was not affected by shot peening since compressive residual stresses were degraded. The fatigue strength at high numbers of load cycles was found to be comparable to the allowable stresses from annealed samples. Compressive residual stresses from shot peening affected the position of the knee point of the S-N curve.
- Residual stress relaxation occurred mainly at the first load cycle in as welded condition. Compressive residual stresses from shot peening were also degraded cyclically.
- The determined improvement factors for annealing are high, for instance compared to those given by [12]. One reason may be the small influence of welding distortion in the tested series. For fatigue improvement of shot-peened welds, there is no recommendation given by IIW [18]. The effect of shot peening is widely known from the literature [19–21] and should be also considered further by IIW in future.

Next, it might be of interest to extend this work to high-strength steels in order to evaluate the effectiveness of tensile and compressive residual stresses at higher yield strength.

**Acknowledgments** The authors would like to thank OSK Kiefer, Oppurg, Germany, for shot peening of specimens used for fatigue testing.

The neutron diffraction measurement was carried out at the Helmholtz Zentrum für Materialien und Energie, Berlin (HZB). The authors thank for the allocation of beam time (HZB proposal MAT01-3215) and the instrument scientists Dr. R.C. Wimpory and Dr. M. Boin for their professional support.

**Open Access** This article is licensed under a Creative Commons Attribution 4.0 International License, which permits use, sharing, adaptation, distribution and reproduction in any medium or format, as long as you give appropriate credit to the original author(s) and the source, provide a link to the Creative Commons licence, and indicate if changes were made. The images or other third party material in this article are included in the article's Creative Commons licence, unless indicated otherwise in a credit line to the material. If material is not included in the article's Creative Commons licence and your intended use is not permitted by statutory regulation or exceeds the permitted use, you will need to obtain permission directly from the copyright holder. To view a copy of this licence, visit <http://creativecommons.org/licenses/by/4.0/>.

## References

1. Wohlfahrt H (1986) Die Bedeutung der Austenitumwandlung für die Eigenspannungsentstehung beim Schweißen (in German). Härtereitechnische Mitteilungen 41:248–257
2. Hensel J, Nitschke-Pagel T, Dilger K (2015) On the effects of austenite phase transformation on welding residual stresses in non-load carrying longitudinal welds. *Weld World* 59:179–190
3. O. Vöhringer (1987) Relaxation of Residual Stresses by Annealing or Mechanical Treatment, “in Advances in Surface Treatments - International Guidebook on Residual Stresses, Pergamon Press, pp. 367–396
4. T. Nitschke-Pagel und H. Wohlfahrt (2000) Residual Stress Relaxation in Welded High Strength Steels under different Loading Conditions, “in International Conference on Residual Stresses 6, 10.-12.07., Oxford, UK
5. Farajian M, Nitschke-Pagel T, Dilger K (2010) Mechanisms of residual stress relaxation and redistribution in welded high-strength steel specimens under mechanical loading. *Weld World* 54(11–12):366–374
6. J. Bergstrom und T. Ericsson (1987) X-Ray Microstructure and Residual Stress Analysis of Shot Peened Surface Layers During Fatigue Loading, “Shot Peening: Science, Technology, pp. 221–230
7. S. Schönborn und T. Nitschke-Pagel, „Einflussgrößen auf die Lage des Abknickpunktes der Wöhlerlinie für den Schwingfestigkeitsnachweis von Schweißverbindungen (in German), “DVS Forschungsvereinigung, Düsseldorf, Germany, 2014
8. R. Olivier und W. Ritter (1979) Catalogue of S-N Curves of Welded Joints in Structural Steels - Part 1: Butt Welds, “DVS Berichte, Düsseldorf
9. R. Olivier und W. Ritter (1979) „Catalogue of S-N Curves of Welded Joints in Structural Steels - Part 2: Transverse Stiffeners, “DVS Berichte, Düsseldorf
10. R. Olivier und W. Ritter (1979) Catalogue of S-N Curves of Welded Joints in Structural Steels - Part 3: Cruciform Joints, “DVS Berichte, Düsseldorf
11. R. Olivier und W. Ritter (1979) Catalogue of S-N Curves of Welded Joints in Structural Steels - Part 4: Longitudinal Stiffeners, “DVS Berichte, Düsseldorf

12. Hobbacher A (2009) Recommendations for fatigue design of welded joints and components. Welding Research Council, New York
13. C. Sonsino (2008) Schwingfeste Bemessung von Schweißverbindungen nach dem Kerbspannungskonzept mit den Referenzradien  $r = 1, 00$  und  $0,05$  mm, “MP Materials Testing, Bde. 1 von 27-8, Nr. Carl Hanser, München, pp. 380–389
14. Hensel J, Nitschke-Pagel T, Dilger K (2014) On welding residual stresses near fatigue crack tips. Adv Mater Res 996:801–807
15. H. Lieurade (2005) Fatigue Improvement of Welded Components by Shot Peening, “in Proceedings of the International Conference on Shot Peening ICSP 9, Mame la Vallee, Paris
16. Maddox S (2010) Fatigue life improvement of steel fillet welds by hammer, needle or shot peening. IIW Document XIII-2327-10. International Institute of Welding, Paris
17. Weich I, Ummenhofer T, Nitschke-Pagel T, Dilger K, Eslami Chalander H (2008) Influence of treatment and loading conditions on the fatigue strength of welds improved by high frequency peening. IIW Document XIII 2218–08. International Institute of Welding, Paris
18. Haagenen P, Maddox S (2011) IIW recommendations on post weld improvement of steel and aluminium Sstructures. The International Institute of Welding, Paris
19. H. Wohlfahrt (1982) Shot Peening and Residual Stresses, “in s Residual Stress and Stress Relaxation, 28th Sagamore Army Materials Research Confernece Proceedings, Sagamore, Plenum Press, pp. 17–92
20. H. Wohlfahrt (1982) Kugelstrahlen und Dauerschwingfestigkeit, “in Proceedings of the 1st International Conference on Shot Peening, Paris
21. J. Heeschen und H. Wohlfahrt (1987) Assessment of the Influence of Shot Peening on the Fatigue Strength of Butt Welded Joints, “Residual Stresses in Science and Technology, Bd. 1, Nr. 1, pp. 23–34
22. A. Hesse (2014) Experimentelle und rechnerische Bewertung der Schwingfestigkeit geschweißter Längssteifen aus S355 unter Berücksichtigung von Eigenspannungen (in German), “M.S. Thesis TU Braunschweig, Braunschweig, Germany